



An urban climate-based empirical model to predict present and future patterns of the Urban Thermal Signal

Ana Oliveira ^{a,*}, António Lopes ^b, Ezequiel Correia ^b, Samuel Niza ^a, Amílcar Soares ^c

^a IN+ Center for Innovation, Technology and Policy Research, Instituto Superior Técnico, Universidade de Lisboa, Portugal

^b Centro de Estudos Geográficos, IGOT - Instituto de Geografia e Ordenamento do Território, Universidade de Lisboa, Portugal

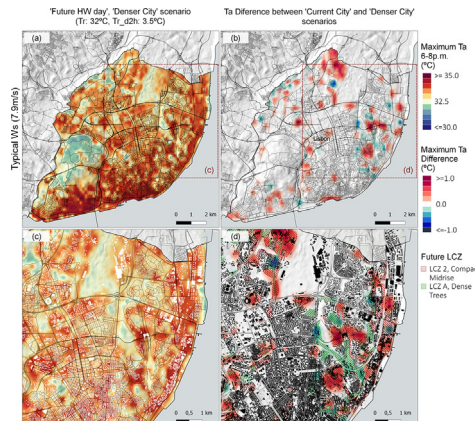
^c CERENA, Instituto Superior Técnico, Universidade de Lisboa, Portugal



HIGHLIGHTS

- Few Urban heat island (UHI) empirical studies include weather-related variability.
- UHI results from the interaction between urban compactness, topography and weather
- Temporal-resolved model can predict the urban thermal signal (UTS) during heatwaves.
- Urban planning and climate change scenarios show which areas are most critical.
- The model is an efficient tool that can be replicated for urban planning adaptation.

GRAPHICAL ABSTRACT



ARTICLE INFO

Article history:

Received 28 March 2021

Received in revised form 28 April 2021

Accepted 8 May 2021

Available online 17 May 2021

Editor: Pavlos Kassomenos

Keywords:

Urban climate change adaptation

Heatwaves

Urban Heat Island

Urban health

Local climate zones

Linear-mixed models

ABSTRACT

Air temperature is a key aspect of urban environmental health, especially considering population and climate change prospects. While the urban heat island (UHI) effect may aggravate thermal exposure, city-level UHI regression studies are generally restricted to temporal-aggregated intensities (e.g., seasonal), as a function of time-fixed factors (e.g., urban density). Hence, such approaches do not disclose daily urban-rural air temperature changes, such as during heatwaves (HW). Here, summer data from Lisbon's air temperature urban network (June to September 2005–2014), is used to develop a linear mixed-effects model (LMM) to predict the daily median and maximum Urban Thermal Signal (UTS) intensities, as a response to the interactions between the time-varying background weather variables (i.e., the regional/non-urban air temperature, 2-hours air temperature change, and wind speed), and time-fixed urban and geographic factors (local climate zones and directional topographic exposure). Results show that, in Lisbon, greatest temperatures and UTS intensities are found in 'Compact' areas of the city are proportional to the background air temperature change. In leeward locations, the UTS can be enhanced by the topographic shelter effect, depending on wind speed – i.e., as wind speed augments, the UTS intensity increases in leeward sites, even where sparsely built. The UTS response to a future urban densification scenario, considering climate change HW conditions (RCP8.5, 2081–2100 period), was also assessed, its results showing an UTS increase of circa 1.0 °C, in critical areas of the city, despite their upwind location. This LMM empirical approach provides a straightforward tool for local authorities to: (i) identify the short-term critical areas of the city, to prioritise public health measures, especially during HW events; and (ii) test the urban thermal

* Corresponding author at: IN+ Center for Innovation, Technology and Policy Research, Instituto Superior Técnico, Universidade de Lisboa, Av. Rovisco Pais 1, 1049-001 Lisboa, Portugal.

E-mail addresses: anappm@tecnico.ulisboa.pt (A. Oliveira), antonio.lopes@campus.ul.pt (A. Lopes), ezequielc@campus.ul.pt (E. Correia), samuel.niza@tecnico.ulisboa.pt (S. Niza), asoares@tecnico.ulisboa.pt (A. Soares).

performance, in response to climate change and urban planning scenarios. While the model coefficient estimates are case-specific, the approach can be efficiently replicated in other locations with similar biogeographic conditions.

© 2021 The Authors. Published by Elsevier B.V. This is an open access article under the CC BY-NC-ND license (<http://creativecommons.org/licenses/by-nc-nd/4.0/>).

1. Introduction

Lisbon is the central city of the Portuguese largest metropolitan area, a dense urban continuum located in the Northern margin of the Tagus river, within the limits of Mediterranean Hot-summer climatic region (Köppen Csa class) (Köppen, 1931; Peel et al., 2007). Its urban climate is strongly affected by the regional climate conditions; in particular, during the summer, the urban heat island (UHI) has been shown to greatly depend on the prevailing near-surface regional wind direction, as well as breezes from the river or from the Atlantic (Alcoforado and Andrade, 2006; Alcoforado, 1992; Oliveira et al., 2021). In Lisbon, mapping the local urban thermal response is of utmost importance, considering recent observed trends and regional climate change prospect, which indicate that extreme heatwave events (HW) are becoming increasingly frequent, more intense, and longer (Beniston et al., 2007; EEA, 2012; Espírito Santo et al., 2014; Giorgi, 2005; Lopes et al., 2018; Mihalakakou et al., 2004; Tolika, 2019). Within cities, such conditions may potentially be aggravated, by the UHI effect (Oke, 1988; Oke et al., 2017), a local air temperature anomaly that results from the urban energy budget characteristics: in artificial and built-up contexts, a large fraction of heat from solar radiation is converted into energy storage and emitted as sensible heat during the night. In addition, latent heat fluxes are reduced, due to fewer vegetation (Chrysoulakis et al., 2018; Feigenwinter et al., 2018; Oke, 1987, 1988; Wang et al., 2010). This potentially aggravates heat exposure, with corresponding consequences, such as the increase in heat-related health problems, outdoor thermal comfort, or energy demand for indoor cooling (Founda and Santamouris, 2017; Geletič et al., 2018, 2021; Heaviside et al., 2016; Levermore and Parkinson, 2017, 2019; Levermore et al., 2015; Li and Bou-Zeid, 2013; Ramamurthy et al., 2017; Tan et al., 2010; Zhou and Shepherd, 2010).

From 2005 to 2014, near-surface air temperature measurements were acquired throughout the city of Lisbon, by the Centre of Geographical Studies - Institute of Geography and Spatial Planning (CEG/IGOT). Since the network's deployment, several follow up studies have been conducted (Alcoforado and Andrade, 2006; Alcoforado et al., 2014; Lopes et al., 2013, 2020b; Oliveira et al., 2021), including statistical models based on linear multivariate regressions to predicting the typical spatial patterns of the UHI intensities, as a response to time-fixed predictors, mostly related with urban morphology, topography and proximity with the Tagus estuary. Therefore, their results were translated into seasonal average/median UHI intensity maps of the city. While these maps have already supported local authorities in addressing urban climate adaptation strategies (Alcoforado and Andrade, 2006; Alcoforado et al., 2009, 2014; CML, 2012; Lopes, 2003; Lopes et al., 2011, 2013, 2018), they did not disclose how the UHI is affected by varying weather conditions, particularly its response to extreme temperatures and wind speed (Reis et al., 2020).

Predictions of the typical/seasonal UHI intensities, based solely on time-fixed or time-averaged predictors, is indeed a frequent methodology in urban climate empirical studies, examples including both the atmospheric canopy layer UHI and the surface UHI (Alcoforado et al., 2014; Ivajnščič et al., 2014; Jiang et al., 2019; Szymanowski and Kryza, 2012; Wicki et al., 2018; Wicki and Parlow, 2017). Some examples also employ individual regression estimates per time step, which results in independent equations (i.e. not related to each other), a strategy that has been mostly adopted in remote sensing studies regarding the surface UHI (sUHI) (Shi et al., 2018; Wicki et al., 2018; Wicki and Parlow, 2017). Less common is the introduction of background (i.e., rural)

weather parameters in these statistical models, for the purpose of disclosing the possible interactions between the time-fixed and the time-varying candidate predictors.

Linear mixed-effects models (LMM), also known as hierarchical models or random effects models, become an advantageous statistical method in this instance, as they allow to simultaneous control for the various data limitations when modelling limited spatial samples, with incomplete but repeated observations, per individual (here, per site) (Bates, 2007; Verbeke and Molenberghs, 2000; Zuur et al., 2009a, 2009b). Lisbon's CEG/IGOT data limitations are due to the unbalanced sampling structure of the data, i.e. few sites with repeated temporal observations, but each one covering different time periods. Such datasets have been described as hierarchical or multilevel data structures, where the repeated measures per unit of observation (here, each site) are expected to be more related to each other, then with those belonging to other units. These limitations imply strong autocorrelation in each site's timeseries, due to its specific urban setting characteristics (e.g. topographic position, urban compactness context). Hence, each urban station's air temperature data has site-specific variances, temporal autocorrelation, and average relation with the candidate predictors (i.e., different slopes and/or intercepts, in a linear model) (Bates, 2007; Zuur et al., 2009a, 2009b). To address these limitations, here, a LMM has been used, allowing to estimate the thermal response of the urban areas, in unsampled space and time. It allows to use all the time series of observations available, while controlling for the difficulties arising from the data structure.

In addition to the above-mentioned methodological constraints to the UHI statistical modelling, a recent study has shown that the summer and HW urban thermal anomaly, in Lisbon, has three case-specific characteristics (Oliveira et al., 2021): firstly, the terrain is a determinant factor, as the city centre (nested in the southernmost and lower altitude riverside area) is topographically sheltered from the prevailing near-surface regional wind, which mostly comes from the north (called 'Nortada'); secondly, these summer northern wind days ('N' days) are not only the most frequent ones (64% cases, in the 2005–2014 time period), but also more likely to be associated with greater air temperatures, including the occurrence of HW events (76% cases, out of 49 HW days, in the same period); and thirdly, the Lisbon's urban-rural air temperature contrasts are characterized by a distinguishable daily cycle, including the existence of a late afternoon peak difference, which increases significantly when northern wind prevails, suggesting strong contributions from local geographical factors, as previously described by (Oliveira et al., 2021).

While the urban cool/heat island (UCI/UHI) effect, by definition and etymology, implies a negative/positive temperature anomaly arising from the urban land use occupation, its magnitudes are often quantified on a daily basis, referring to either the UCI or UHI periods of the day. Typically, the UHI is shown to be a nocturnal effect, which magnitude peaks shortly before sunrise, and can be attributed to the urban occupation. However, following the analytic framework from Lowry (1977), also adopted by Oke et al. (2017), a given weather variable (V_M) results from sum of three components: (i) the 'background' macroclimate of region (V_B), (ii) the contribution from geographic/landscape factors (e.g. relief, water bodies) (V_L), and (iii) the contribution from human activities and occupation (V_H) (e.g. urban land cover). According to Oke et al. (2017), the UHI corresponds to the V_H component, i.e., the contribution attributable to the human activities/occupation; accordingly, the authors suggest avoiding the usage of the UHI terminology when considering settings where complex local geographical/landscape control

factors exist, such as topography or coastal proximity, as these are likely to determine the existence of a 'spurious' positive urban-rural air temperature difference that cannot be attributable solely to the urban occupation itself. In fact, in Lisbon, the hourly quantification of the urban-rural air temperature differences shows a different infra-daily cycle that strongly suggest the local existence of such complex contrasts between the V_L component in the upwind rural plateau area, and the downwind riverside urban setting. Accordingly, Lisbon's hourly urban-rural air temperature, referred in that study (Oliveira et al., 2021) as the Urban Thermal Signal (UTS), is equivalent to the cumulative contribution of both V_L and V_H components, due to the absence of alternative reference non-urban stations where the landscape/topographic contribution would be the same as within the city. Hence, the UTS is different from the UHI intensity, which should only account for the human-induced V_H component (Lowry, 1977; Oke et al., 2017). The quantification of the UTS hourly intensities and rate of change has allowed to: (i) classify which moments of the day show significant negative or positive UTS peaks (phase change), and which periods can be characterized as either phase transition or stable periods; and (ii) quantify the UTS intensity (and corresponding statistical spread) during those stages. From this rationale, Lisbon's UTS daily cycle becomes apparent, characterized by six daily stages, as depicted in Fig. 1 (Oliveira et al., 2021): (i) Stage 1, the nocturnal stable UTS period during which positive thermal anomalies have minimal hourly changes; (ii) Stage 2, a morning transition period, during which the UTS reduces by more than 0.2 °C per hour, becoming negative at the city centre; (iii) Stage 3, when the minimum daily UTS intensity is reached; (iv) Stage 4, the afternoon transition period, when the UTS increases by more than 0.2 °C per hour; (v) Stage 5, when the late afternoon peak UTS intensity is reached; and (vi) Stage 6, the evening stabilizing UTS period, transitioning to Stage1.

The UTS stages 1 (nocturnal stable UTS) and 5 (late afternoon peak UTS) are the most relevant for intra-urban heat exposure, i.e., they correspond to periods/moments of the day during which an UHI effect has previously been reported, at the city centre.

Accordingly, the LMM developed in this study aims to estimate the UTS spatial patterns during these positive UTS stages. The median UTS is considered the representative daily statistical summary of Stage 1, quantifying the stable UTS intensity from 11 p.m. to 6 a.m.; and the daily maximum UTS, from 6 p.m. to 8 p.m., becomes the appropriate

statistic criteria to depict the momentaneous nature of the daily Stage 5 UTS peak. These median and maximum UTS are modelled in response to the interactions between the regional weather predictors and the built-up and geographical factors. The model focuses on the 'N' summer days, when regional northern winds predominate (as registered at the Airport station), during which HW are more likely to occur, and an urban air temperature positive anomaly is potentially more harmful, aiming to disentangle the contributions from weather variables as they interact with the local terrain and built-up urban fabric (Oliveira et al., 2021).

2. Data and methods

2.1. Single-level model (LM) versus linear-mixed model (LMM)

In urban climate-related studies, LM models have been widely implemented, granting straightforward interpretations of the corresponding coefficient estimates (Alcoforado and Andrade, 2006; Alcoforado, 2013; Ivajnič et al., 2014; Lopes et al., 2013; Shi et al., 2018; Szymanowski and Kryza, 2012; Wicki et al., 2018; Wicki and Parlow, 2017). However, a LM requires a set of conditions to be met: firstly, the response variable (here, the UTS intensity), must be a linear function of the explanatory variables used; secondly, residuals must be independent, i.e. without autocorrelation; and thirdly, residuals variance must be constant, across observations (Zuur et al., 2009a, 2009b).

Here, the number of sites where urban air temperature (T_u) has been measured is very small: there are only 9 sites available from the CEG/IGOT network, but from those, only 6 ensure a consistent and partially overlapping time series. This poses serious constraints in that the sampling is limited: from the usable sites, each one represents a different class of land cover (with the exception of Restauradores and Saldanha sites, both LCZ 2) (see Table A.1 and Figs. A.1 and A.2 in the Supplementary Materials, Appendix A), but also unique geographic settings, and these characteristics affect each site's time series data structure, namely its variability, independence of observations, and temporal autocorrelation, violating the previously mentioned LM assumptions (Zuur et al., 2009a, 2009b).

LMM, also known as multilevel models, random coefficients models, or hierarchical models, solve some of the above-mentioned issues, by

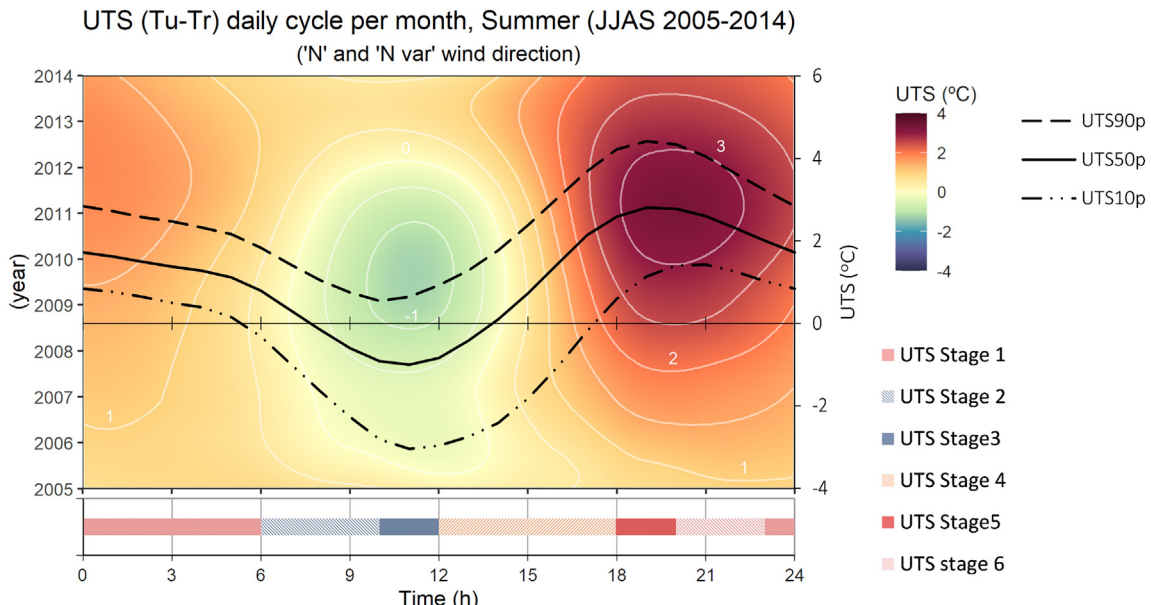


Fig. 1. UTS daily cycle in Lisbon, adapted from (Oliveira et al., 2021): line plot displays the median, the 90th and the 10th percentiles of the hourly UTS intensity (UTS50p, UTS90p and UTS10p, respectively) at the Lisbon's city centre (Restauradores), together with the corresponding heatmap, per year; bellow, the schematic diagram depicts the corresponding UTS daily cycle stages. In this study, two stages are considered: the daily median nocturnal UTS intensity, from 11 p.m. to 6 a.m. (Stage 1); and (iii) the daily late afternoon maximum UTS intensity, from 6 p.m. to 8 p.m. (Stage 5).

simultaneously modelling the overall model coefficients (city level, or level 0) and the grouping structure of the observation sites (Gelman and Hill, 2006; Zuur et al., 2009a, 2009b) (temporal and spatial); this allows to introduce the hierarchical structure of the acquired data, such as grouping each CEG/IGOT station time series, at the inner level of the LMM structure, which is appropriate given the repeated observations (Gelman and Hill, 2006; Zuur et al., 2009a, 2009b). Here, each site's time series has a varying number of observations and time spans. These conditions affect the possibility of using simpler models, such as repeated measures ANOVA, as the overlapping time series would be quite short (less than 50% of observations), and with many gaps.

Due to the above-mentioned limitations, previous studies on Lisbon's UHI have only produced models of the temporal aggregated UHI intensity, as a function of temporal invariant explanatory variables, such as built-up geometry indices and geographic factors (Alcoforado et al., 2014; Lopes et al., 2013), explaining their average effect on the median UHI intensity. However, this approach does not reveal how these factors interact with daily varying weather conditions, to explain the great spread of variance detected, at each of the urban sites. Eq. (1) represents the linear regression model (Gelman and Hill, 2006):

$$y_i = \beta_0 + \beta_1 x_{i1} + (\dots) + \beta_k x_{ik} + \varepsilon_i, \text{for observations } i = 1, \dots, n \quad (1)$$

where y_i is the response variable, β_0 is the intercept, x_{i1} to x_{ik} are the predictors (or explanatory variables of interest), β_1 to β_k are the effects each predictor on the response variable, and ε_i is the error term, with normal distribution. By comparison, a LMM can have either different intercepts or different intercepts and slopes, per each of the groups from the nesting structure. As a result, there is an observation-level regression and a group-level regression (here, a regression for the city, and a regression per site, computed simultaneously). Eq. (2) shows a LMM model with random intercept and slope (response variable as y_{ij}), as used in this study, and Eqs. (3) and (4) show the corresponding equations predicting the intercept (β_{0j}) and slope (β_{1j}):

$$y_{ij} = \beta_{0j[i]} + \beta_{1j[i]} x_{i1} + (\dots) + \beta_{kj[i]} x_{ik} + \varepsilon_i, \text{for observations } i = 1, \dots, n \quad (2)$$

$$\beta_{1j} = a_1 + b_1 u_j + \eta_{j1}, \text{for observation groups } j = 1, \dots, k \quad (3)$$

$$\beta_{2j} = a_2 + b_2 u_j + \eta_{j2}, \text{for observation groups } j = 1, \dots, t \quad (4)$$

where the j subscript corresponds to each different group - here, each CEG/IGOT site. The varying intercept (β_{0j}) and slopes (β_{1j} to β_{kj}) are modelled at the first and second 'inner' levels (Eqs. (3) and (4)), where β_{1j} and β_{2j} depict the group-specific estimated coefficients $a_{1/2}$ and $b_{1/2}$, with corresponding predictor(s) (u_j) and second level errors (η_{j1} and η_{j2}), for group-level observations k and t . Both the a and b (per site) parameters are controlled by the hyperparameters of the upper-level fixed structure of the model, characterizing each site's distinct variance, auto-correlation and/or random effect over the predictor (Gelman and Hill, 2006; Zuur et al., 2009a, 2009b).

In this study, the LMM has set of fixed effects that correspond to the explanatory variables from which to predict the UTS intensity in the city of Lisbon, and a three-levels grouping structure, as follows:

- At the 'city-level', or upper level (level = 0), the LMM estimates the UTS intensity response to the fixed-effects (predictors), and their individual contributions. This model can be used to predict the gridded results across the city, irrespective of the time of the day.
- At the 'city and UTS stage-level', or mid-level (level = 1), the LMM estimates two different UTS intensity response functions, one per each period of the day (the UTS Stage 1, nocturnal stable UTS, and the UTS Stage 5, late afternoon peak UTS). In result, this model can be used also to predict the gridded results across the city, at specific UTS daily cycle stages.

3. Finally, at the 'site-level', or lower level (level = 2), the LMM estimates each site-specific UTS intensity response function, accounting for its site-specific time-series data structure (variance, auto-correlation). Hence, while this inner level equations provide the greatest agreement, its results can only be used to predict the UTS in each site location.

2.1.1. Response variable

As previously mentioned, the response variable, UTS, has positive intensities during two specific periods of the day: the stable nocturnal period, UTS Stage 1, and the late afternoon maximum, UTS Stage 5. These daily statistics are calculated from the hourly UTS dataset from a previous study (Oliveira et al., 2021), focusing on the UTS daily cycle during the summer and HW days, considering the extended summer period, spanning from June to September (JJAS), from 2005 to 2014. The UTS intensity corresponds to the hourly urban-rural air temperature differences and is calculated per each site of the CEG/IGOT mesoscale weather observation network, as per (Oliveira et al., 2021) and shown in Eq. (5). The urban mesoscale observation network included 9 temperature/relative humidity probes, with Tiny Tag Plus (Gemini) data loggers, installed on public lighting poles, at 3.5 m height, inside radiation protection shields, following previous advice by T.R. Oke, during an ongoing urban climatology project, and testing routines were established to ensure data quality (see Alcoforado and Andrade, 2006; Alcoforado et al., 2014 for further details).

$$UTS = Tu - Tr \quad (5)$$

where Tu refers to the air temperature observed in each urban site of CEG/IGOT network, and Tr is air temperature observed at the Lisbon Airport meteorological station, both at a specific hour of the day. The need for a UTS designation comes from the fact that, in Lisbon, these hourly urban-rural differences reflect both the contributions from the local geographical/landscape controlling factors (V_L , per Lowry (1977)) and the urban occupation/human activities (V_H , per Lowry (1977)), as detailed in Section 1.

The input data was acquired between 2005 and 2014, at 3.5 m height (Alcoforado et al., 2014), and followed strict installation procedures. A detailed description of the sensors, data acquisition and quality control can be found in (Alcoforado et al., 2007, 2014; Lopes et al., 2013; Oliveira et al., 2021). The reference background weather station considered was the Lisbon's Airport (AIR), from the Integrated Surface Database – Global Hourly Observations (ISD/GH), available at the National Centers for Environmental Information of the National Oceanic and Atmospheric Administration (NOAA) (Lott, 2004), to ensure results comparability with previous studies. Two additional sites from the ISD/GH database, the Geophysics Institute (GEO) and the Lisbon / Gago Coutinho (LGC), were used to validate predictions, out of the temporal scope of the input data. Data from the ISD/GH sites was retrieved for the 2020 summer, from June to August (September data was unavailable at the time). All the measurement sites are described in Table A.1, in the Supplementary Materials, Appendix A. Additional information on the UTS calculation and definition is available in (Oliveira et al., 2021).

In a previous study, it was shown that northern wind days ('N' days) had statistically significant contrasting UTS profiles, characterized by greatest late afternoon and nocturnal UTS intensities, at the city centre (Restauradores site), as well as greater daily maximum air temperature (Tx) values, at the Airport site. In addition, prevailing regional north wind conditions were shown to be associated with more than half of the HW days (Oliveira et al., 2021).

As such, here, only the northern wind days ('N' and 'N var' days) from the previous study were considered. Within this group of days, the previous study also highlighted the existence of a consistent UTS daily cycle, especially at the city centre, comprising 6 stages, as described in Section 1. From those stages, the UTS is consistently positive

in two cases: (i) in Stage 1, stable nocturnal UTS, characterized by very low hourly changes of intensity; and (ii) in Stage 5, late afternoon peak UTS, the momentaneous daily maximum intensity. Hence, the hourly UTS intensities were aggregated into two daily values, accordingly: (i) the daily median UTS intensity, from 11 p.m. to 6 a.m. (Stage 1); and (iii) the daily maximum UTS intensities, from 6 to 8 p.m. (Stage 5). These stages are depicted in Fig. 1, Section 1.

2.1.2. Weather variables as temporal predictors

Hourly meteorological observations at the reference Airport site were used as time-varying predictors. This data is available at the ISD/GH database (Lott, 2004), and includes the 2 m air temperature (Tr) and wind speed (Ws) observations. Both were also aggregated per each of the two main UTS stages, using the same statistical criteria: (i) Stage 1, the nocturnal stable UTS (daily median Tr and Ws, from 11 p.m. to 6 a.m., per site); and (iii) Stage 5, the late afternoon peak UTS (daily maximum Tr and Ws, from 6 p.m. to 8 p.m., per site).

Finally, in the study from (Oliveira et al., 2021) a 2-hour lag was detected, between the air temperature curves of the urban and rural sites. Accordingly, a positive and significant correlation was detected, between the urban station's air temperatures, and the air temperature at the airport, 2 h earlier, as the former lags 2 h behind ($R^2 = 0.94$, p -value < 0.001). Hence, the air temperature change in 2-hours, at the airport (Tr_d2h), was calculated as per Eq. (6), and used in the model as predictor.

$$Tr_d2h_{(h=0)} = Tr_{(h=-2)} - Tr_{(h=0)} \quad (6)$$

where h is time difference between Tr observations (here, 2 h).

2.1.3. Geographic variables as spatial predictors

The geospatial information was gathered from several open-data sources. These included: (i) urban built-up properties, as per the Local Climate Zones classification (LCZ) (Oliveira et al., 2020a, 2020b); and (ii) natural geographical factors, such as altitude, from a digital elevation model (DEM) (Team, 2009). The LCZ classification was converted into LCZ-equivalent Bowen Ratio (LCZ_{BR}) values, as per (Oke et al., 2017; Stewart and Oke, 2012) reference values – these are shown in Table A.2, in the Supplementary Materials, Appendix A.

In addition, the DEM dataset was transformed into the topographic exposure index, considering the north-northwest wind direction (TopexNNW), as it is the most frequent within the 'N'/N var' days group (Oliveira et al., 2021). The TopexNNW algorithm was implemented in ArcGIS PRO software, version 2.3, through the raster calculator tool, following the formulation by Chapman, 2000. To calculate the maximum angle of occultation/exposure, for each point, the angle of the elevation of the topography is calculated in sequential distances (each 100 m) until a 2 km radius is reached, in a given cardinal compass direction; the maximum occultation angle is then chosen as the Topex index, with positive (negative) values corresponding to the average shelter (exposure) levels, per pixel. These values correspond to the maximum terrain obstruction angle (in radians), in a 2.0 km distance, per a given cardinal direction. In Lisbon, the TopexNNW is strongly correlated with DEM itself (Pearson's coefficient greater than 0.8, p -value < 0.001), and thus the latter was excluded from the model.

Further land cover/land use layers were tested, including building height information (European Environment Agency (EEA), 2018a), Tree Cover Density (TCD) (European Environment Agency (EEA), 2018b), and imperviousness density (IMD) (European Environment Agency (EEA), 2018c); however, all were found to be strongly correlated with the LCZ_{BR} variable (Pearson's coefficients greater than 0.8, p -value < 0.001, on every case). Finally, land cover classification and urban development regulatory constraints were retrieved from Lisbon's Municipal Master Plan (LMP) (CML, 2012). Original categories from the LMP were reclassified according to the future land-use/land-cover (LULC) regulation: (i) 'existing built-up areas' and 'existing

green areas', where urban development/green areas are already 'consolidated', and not allowed to change; and (ii) 'future built-up areas' and 'future green areas', where new or denser urban development/green areas are permitted/expected. Fig. A.2 in the Supplementary Materials, Appendix A, depicts these geographic variables, together with the location of CEG/IGOT (training and testing) and ISD/GH (validation) sites.

2.1.4. Modelling protocol

For quality control assessment (QA) of the input data, two procedures were implemented in the original hourly dataset: firstly, the Minimum Covariant Determinant method, at the 50 level (MCD50), was used to identify observations with abnormal air temperature differences between the urban (Tu) the Lisbon Airport site (i.e. Tr); the method aims to identify outliers in multivariate time series, based on their covariances, and was implemented in R (R Development Core Team, 2011), version 4.0.2, following (Leys et al., 2018) available code; secondly, the interquartile range (IQR) was applied to the hourly UTS intensities, identifying additional UTS outliers from the series (i.e., values outside the $\pm 1.5 \times IQR$ range). The latter method was also implemented in R (R Development Core Team, 2011), version 4.0.2, and followed the method used in the Climpact2 tool (Alexander and Herold, 2016; L. and N., 2015). Out of 74,587 hourly observations, 9% were classified as outliers and excluded from the time series (summary available in Table A.3, Supplementary Materials, Appendix A).

After QA, the complete daily time series of 'N'/N var' days was split into training and testing datasets, ensuring that (i) both had equivalent data distributions, and (ii) temporal continuity was kept (i.e., no random sampling was used). Thus, the summer (JJAS) observations of 2005, 2008 and 2014 were withheld from the training dataset, and used for testing only. For validation purposes, the 2020 summer data available from the ISD/GH stations was used. Only days with prevailing northern wind were used, from the 2020 validation dataset, using the same classification criteria as in (Oliveira et al., 2021), i.e., an 80% of the day (hourly observations) threshold to discard non-northern wind days.

Both the Akaike's information Criterion (AIC) and Bayesian information criterion (BIC) are used to evaluate the performance throughout the modelling protocol, instead of the coefficient of determination (R^2), due to the limitations in using the latter to appropriately evaluate LMM (Bates et al., 2015; Zuur et al., 2009a, 2009b). The smaller the AIC value, the better the model's performance.

The daily UTS intensity (median, in Stage 1, and maximum, in Stage 5) was modelled as the response to the interactions between the background weather conditions and non-time varying geographical/built-up characteristics previously mentioned. The hierarchical structured of the LMM included the UTS stages 1 (nocturnal median) and 5 (late afternoon maximum), in level 1, and each site, in level 2. The model was ran in R (R Development Core Team, 2011), version 4.0.2, using the lme4 packages (Bates et al., 2007, 2015). The model specification is shown in Eq. (7), as follows:

$$UTS = \beta_{0j,k} + \beta_{1j,k[i]} \times Tr_d2h + \beta_{2[i]} \times LCZ_{BR} + \beta_{3[i]} \times Tr_d2h \times LCZ_{BR} \\ + \beta_{4,j,k[i]} \times Ws + \beta_{5[i]} \times Topex_{NNW} + \beta_{6[i]} \times Ws \times Topex_{NNW} + \beta_{7[i]} \\ \times Tr + \eta_{j,k} + \varepsilon_i, \text{for observations } i = 1, \dots, n \quad (7)$$

where $\beta_{0j,k}$ represents the intercept, which varies per j site and k UTS Stage, $\beta_{1j,k[i]}$ and $\beta_{4,j,k[i]}$ are the varying slopes (per j site and k UTS Stage, as well) of the corresponding weather variables Tr_d2h and Ws , and $\beta_2, \beta_3, \beta_5, \beta_6$, and β_7 are the predictors with fixed slopes. The error terms are the overall error ε_i , and the varying UTS Stage/site errors $\eta_{j,k}$. A detailed description of the sequential steps of the protocol, as well as the list and corresponding R syntax of the models, estimators used, and AIC results are presented in Section 4 of the Supplementary Materials, Appendix A. An autocorrelation structure was added, per site and UTS stage, considering a 1-day lag, (i.e., a 1st order autoregression, that relates the predictions for a given day with the previous day's prediction).

In addition to following with the protocol to assess the fixed effects significance, the intercept's significance was also tested. To test this hypothesis the Regression Through the Origin (RTO) LMM (LMMf0) was compared to the final/best performing non-RTO LMM (LMMf), and the intercept tested for significance and confidence intervals. The level 0 intercept was shown to be non-significant, and numerically not meaningful (i.e., small values and varying from positive to negative values, per nesting level). Finally, spatial patterns in the residuals were also tested for spatial autocorrelation, but no significant results were detected, which was expected given the very small number of sites. The results comparison, and assumptions inspection plots are available in Section 5 of the Supplementary Materials, Appendix A.

3. Results

3.1. Model estimates and performance

Table 1 reports the final LMMf0 results: the Fixed Effect, refer to the coefficient estimates for each predictor term introduced in the model (including the interaction terms), considering no intercept, at the 'city-level' (level = 0), together with the corresponding confidence intervals (CI, at the 95% level) and significance levels, as per the LMM modelling protocol (Zuur et al., 2009a, 2009b). The Random Effect report the characteristics of each grouping level, namely its variance, number of observations per group, and interclass correlation level (ICC).

All the fixed effects are shown to be significant, at the 99% level. Estimates and confidence intervals show that, on average, at the city and UTS Stage level, the greatest positive contribution to the UTS intensity comes from the Tr change in the last 2 h (Tr_d2h), given the 0.271 coefficient [95% CI: 1.55–0.38] as well as from the LCZ_{BR} urban compactness indicator, with a 0.283 estimate [95% CI: 0.160–0.406]. The interaction term between these predictors also enhances the UTS intensity, in most compact locations [0.043, 95% CI: 0.014–0.072].

Conversely, the wind speed influence (Ws predictor) only becomes meaningful through the interaction with the topography. The interaction between the TopexNNW and Ws variables is thus shown to contribute to the UTS, with an estimated effect of 0.135 [95% CI: 0.065–0.20], also positive at the City and UTS Stage levels (see level 0 estimates in **Table 1**, and level 1 estimates in Eqs. (8), and (9)). Thus, the positive or negative contribution of the Ws to UTS is determined by the value of NNW wind shelter at each site: in locations that are exposed to NNW winds, TopexNNW assumes a negative value which is then multiplied by wind speed. In such cases, there is

Table 1
Linear Mixed-Effects Model LMMf0 estimates (level = 0).

| Predictors | Estimates | CI (95%) | | Significance ¹ |
|--|-------------|----------|--------|---------------------------|
| | | Lower | Upper | |
| Fixed effects | | | | |
| Tr_d2h | 0.271 | 0.155 | 0.388 | ** |
| LCZ _{BR} | 0.283 | 0.160 | 0.406 | ** |
| Ws | -0.030 | -0.066 | 0.005 | ** |
| TopexNNW | 0.376 | -0.271 | 1.022 | ** |
| Tr | -0.036 | -0.044 | -0.028 | *** |
| Tr_d2h × LCZ _{BR} | 0.043 | 0.014 | 0.072 | *** |
| Ws × TopexNNW | 0.135 | 0.065 | 0.205 | *** |
| Random effects | | | | |
| σ^2 | 5.0 | | | |
| τ_{00} site/UTS Stage | 0.09 | | | |
| τ_{11} site/UTS Stage Tr_d2h | 0.01 | | | |
| τ_{11} site/UTS Stage Ws | 0.04 | | | |
| Nr. UTS Stage | 2 | | | |
| Nr. site/UTS Stage | 14 | | | |
| ICC site/UTS Stage | 0.91 | | | |
| Observations | 3831 | | | |
| Marginal R ² / Conditional R ² | 0.11 / 0.92 | | | |

¹ Significance: * p-value < 0.05; ** p-value < 0.01; *** p-value < 0.005.

multiplicative effect of Ws determining the UTS reduction. Contrariwise, topographically sheltered areas (positive TopexNNW) have a positive UTS contribution from wind speed. However, at the site level, the confidence intervals of these predictors are wider, thus one cannot exclude that their contribution to the UTS is more site-specific than fixed, throughout the city. Finally, the overall air temperature level was previously noted for not having a significant positive impact in the UTS intensity in Lisbon, with similar statistical UTS percentile curves during both HW and non-HW conditions (Oliveira et al., 2021). Here, the model reveals a significant, albeit weak, negative contribution to the UTS, by a factor of 3.6. In other words, a 10 °C increase in the nocturnal median or late afternoon maximum air temperature, at the Lisbon Airport, implies a 0.36 °C UTS reduction (all other variables remaining equal).

At the "city and UTS Stage-level" (level = 1), Eq. (8) (nocturnal daily median UTS) and Eq. (9) (late afternoon daily maximum UTS) show the equivalent coefficient estimates, as a LMM output function, at the UTS Stage level; these equations are the ones used in predicting the UTS intensity throughout the city, during each UTS Stage (see Sections 3.1). From the comparison between the level 0 and level 1 estimates, the intercept and the nested weather predictors are shown to change only very slightly. This shows that the fixed effects estimates, subjected to the hierarchical structure (i.e., the weather variables) are not greatly affected by the time of the day. The site-level (i.e., level 2) estimates maintain the same positive values, on every case (see supplementary Materials, Appendix A).

UTSLisbon, UTS stage 1 (nocturnal median)

$$= -0.045 + 0.237 \times Tr_d2h + 0.283 \times LCZ_{BR} + 0.043 \times Tr_d2h \\ \times LCZ_{BR} + (-0.025) \times Ws + 0.376 \times TopexNNW + 0.135 \times Ws \\ \times TopexNNW + (-0.036) \times Tr \quad (8)$$

UTSLisbon, UTS stage 5 (late afternoon maximum)

$$= 0.066 + 0.322 \times Tr_d2h + 0.283 \times LCZ_{BR} + 0.043 \times Tr_d2h \\ \times LCZ_{BR} + (-0.039) \times Ws + 0.376 \times TopexNNW + 0.135 \times Ws \\ \times TopexNNW + (-0.036) \times Tr \quad (9)$$

Regarding the model's performance, the estimates reveal a very strong inter-class correlation (ICC), at the site level (see **Table 1**): statistically, this indicates that there is a lack of spatial sampling, throughout the city, i.e., that a great proportion of the temporal variability is site-specific, and not explainable solely by the city-level model. This finding was expected as the number of sites available is quite limited, and therefore each one is representative of specific characteristics that are not measured elsewhere. Nonetheless, at the inner level, the coefficients have similar signs and magnitudes on almost every case (see Table A.7 in the Supplementary Materials, Appendix A). In addition, the residual results, shown in **Table 2**, indicate that the level-1 model has an adequate performance to estimate the city-level variance of the UTS intensities, during each UTS Stage, in the testing and validation datasets.

The median nocturnal UTS intensity predictions have the best performance - its Mean Absolute Error (MAE) is lower than 0.5 °C, on every case (training, testing and validation subsets). On the other hand, the late afternoon daily maximum UTS has larger residuals, with an average MAE of 0.8 °C. Results from the validation dataset ('N' days, in the summer 2020) have equivalent accuracies. Despite the strong ICC, there is only a slight residuals reduction, when using the site-specific coefficients (level = 2). The expanded version of **Table 2**, depicting the residuals, by site and LMMf0 levels is available in Tables S8 and S9, in the Supplementary Materials, Appendix A.

3.2. Model predictions and spatial patterns of the UTS

3.2.1. Historical time-series

To assess the spatial patterns of the LMMf0 model, a grid of regularly spaced points, set apart by 100 × 100 m, was used to sample the time-fixed predictors, LCZ_{BR} and TopexNNW, throughout the city of Lisbon.

Table 2

Comparison of the LMMf0 model residuals, in the training, testing and validation subsets.

| LMM _{f0} Model Level | Training Subset (JJAS, 2006–2014 ^a) N = 3831 | | | | Testing Subset (JJAS, 2005, 2008 and 2011) N = 2451 | | | | Validation Dataset (JJA, 2020) N = 98 | | | |
|--------------------------------------|--|------|--|------|---|------|--|------|---|------|--|------|
| | UTS Stage 1, Nocturnal Stable UTS | | UTS Stage 5, Late Afternoon Peak UTS | | UTS Stage 1, Nocturnal Stable UTS | | UTS Stage 5, Late Afternoon Peak UTS | | UTS Stage 1, Nocturnal Stable UTS | | UTS Stage 5, Late Afternoon Peak UTS | |
| | MAE | RMSE | MAE | RMSE | MAE | RMSE | MAE | RMSE | MAE | RMSE | MAE | RMSE |
| City, UTS Stage level (level = 1) | 0.47 | 0.60 | 0.80 | 0.94 | 0.47 | 0.61 | 0.93 | 1.10 | 0.26 | 0.37 | 0.84 | 1.10 |
| Site Level (level = 2) | 0.43 | 0.55 | 0.65 | 0.79 | 0.45 | 0.59 | 0.94 | 1.14 | n.a. | n.a. | n.a. | n.a. |

^a Except testing years (JJAS, 2005, 2008 and 2011).

Two time-series of gridded LMMf0 predictions (at level = 1) were computed, in result: (i) the complete 2005–2014 time series of summer 'N' days; and (ii) the summer 2020 'N' days. These gridded predictions are available upon request to the authors. Fig. 2 shows the maps of the 50th UTS intensity percentile (UTS50p), from the 2005–2014 period, corresponding to the daily nocturnal median (1), and late afternoon maximum (5) UTS Stages. The spatial pattern overall agrees with previous studies (Alcoforado and Andrade, 2006; Alcoforado et al., 2014; Lopes et al., 2020b), albeit with much greater detail (see zoom details in Fig. 2).

Lisbon's greater positive UTS intensities are shown to follow a spectacular spatial pattern that accompanies the main valleys (due to the topographic shelter contribution), and the urban development axis (due to addition of the built-up occupation contribution). While previous studies have already indicated the 'finger-like' pattern along the two structuring avenues of the city ('Liberdade' and 'Almirante Reis'), in the LMMf0 model predictions the UTS intensity is enhanced by the topographic shelter contribution, mostly noticeable in downwind locations, and even in the absence of significant urban density. In most developed areas (LCZ classes 1–3), such as the city centre (Restauradores site), the local UTS intensities are further increased by the contribution of urban compactness (LCZ_{BR} predictor). Hence, under northern wind conditions (median: 5.0 m/s), a positive UTS is present during the night, with a median 1.3 °C intensity, similar to the 1.5 °C stated in previous studies (Alcoforado et al., 2014; Lopes et al., 2020b).

Positive UTS intensities of at least 1.0 °C are found along the riverside, from the city centre (Restauradores site) up to the western limit of the city (Belém site), as the result from the overlapping contributions of wind shelter and built-up density. In the westernmost area, the positive UTS intensities enter further inland, accompanying the terrain's gentler slopes. Urban parks are easily noticed as cool spots in city, as shown in Fig. 2 zoom details. While the forest area of the Monsanto is easily noticed, due to its size, the LMMf0 is also able to depict, for the first time, the cooling effect of the several smaller urban green areas such as the Eduardo XVII Park, the Botanical Garden, Lisbon's Zoo and even Cemeteries such as Prazeres. Fig. 2 also shows the model results corresponding to the daily late afternoon peak UTS predictions, a daily UTS Stage which has not been address in previous regression-based modelling attempts (Alcoforado and Andrade, 2006; Alcoforado et al., 2014). Its results show a similar pattern to the nocturnal UTS map, although with significantly greater intensities, reaching up to 3.5 °C, at the city centre and western riverside areas. The contrast between upwind and downwind locations is also accentuated, which was expected as wind speed is the greatest during this period of the day (median: 7.9 m/s) (Oliveira et al., 2021).

The LMMf0 model is also able to predict, for the first time, daily patterns of the UTS, in response to weather conditions. To better illustrate this application, predictions corresponding to the warmest day during and HW event, (16 of July 2020), is shown in Fig. 2. During this HW event, air temperatures surpassed the 90th percentile of the

1981–2010 30-years period, during 3 consecutive days, at the Lisbon Airport. In the warmest HW day, the 16th of July, absolute air temperatures were 36.3 °C (late afternoon maximum, from 6 to 8 p.m.) and 28.4 °C (nocturnal median, from 11 p.m. to 6 a.m.).

During the warmest day of the HW event, the nocturnal UTS intensity becomes weaker (up to 1.0 °C), and the positive intensities cover a smaller area of the city. However, the spatial pattern is similar to that of UTS50p maps. Conversely, during the late afternoon peak UTS Stage, the UTS intensity is similar, in response to the greater air temperature rate of change (Tr_d2h) interaction with the LCZ_{BR} predictor, enhancing the contrast between built and non-built-up areas. During this specific HW day, the weaker nocturnal UTS intensities should not be disregarded as it translates into an overall air temperature that surpasses the 38.5 °C, during the late afternoon period, and remains 29.5 °C, during the night, at the city centre. Hence, the model provides a useful local-level decision-supporting tool to evaluate the daily relative heat exposure differences, across areas of the city, one that can be merged with economic and social data to provide daily vulnerability assessments, from a meso-scale perspective.

3.2.2. Weather and urban planning scenarios: Present and future

To disclose the model's sensitivity to each of the time-varying weather predictors, i.e. the UTS response to changes in wind speed, air temperature or air temperature changes, separately, as well as identifying potential impacts of increasing the built-up compactness in the city, predictions from the LMMf0 model (level = 1) were calculated, considering a group of 50 scenarios - 25, per UTS Stage. These are based on the same 100 × 100 m regular grid of geographical inputs, but the weather predictors correspond to predetermined values depicting the time series median and lower/upper extremes (5th and 95th percentiles, considering the Airport site 1981–2010, 30-years period, retrieved from the ISD/GH. Two additional 'worst-case-scenarios' of climate change were considered, for 2081–2100 period, using the percentile values of both air temperature and HW intensity, as per (Parente et al., 2018), keeping the Airport site as the regional reference. According to regional climate change prospects, HW days are very likely to become more frequent and intense, which may pose local communities at risk of thermal stress (EEA, 2012; Espírito Santo et al., 2014; Lopes et al., 2018). While the UTS intensity has previously been shown not to be significantly changed during recent cases of HW days, in Lisbon, (refer to Oliveira et al., 2021) its presence is still detected, potentially enhancing human thermal exposure by more than 2.5 °C, during the late afternoon peak period of the day, in the most compact areas of the city. In addition, regional climate change prospects have pointed out that air temperature is the weather variable more likely to affect local human thermal discomfort, as the summer relative humidity is typically lower (dry summer climate), and no significant changes were suggested (Lopes et al., 2018). Accordingly, two future scenarios are considered, depict climate change HW conditions together with two alternative levels of urban density: in one scenario, the current built-up occupation was considered, while in the other the UTS response to an urban 'densification'

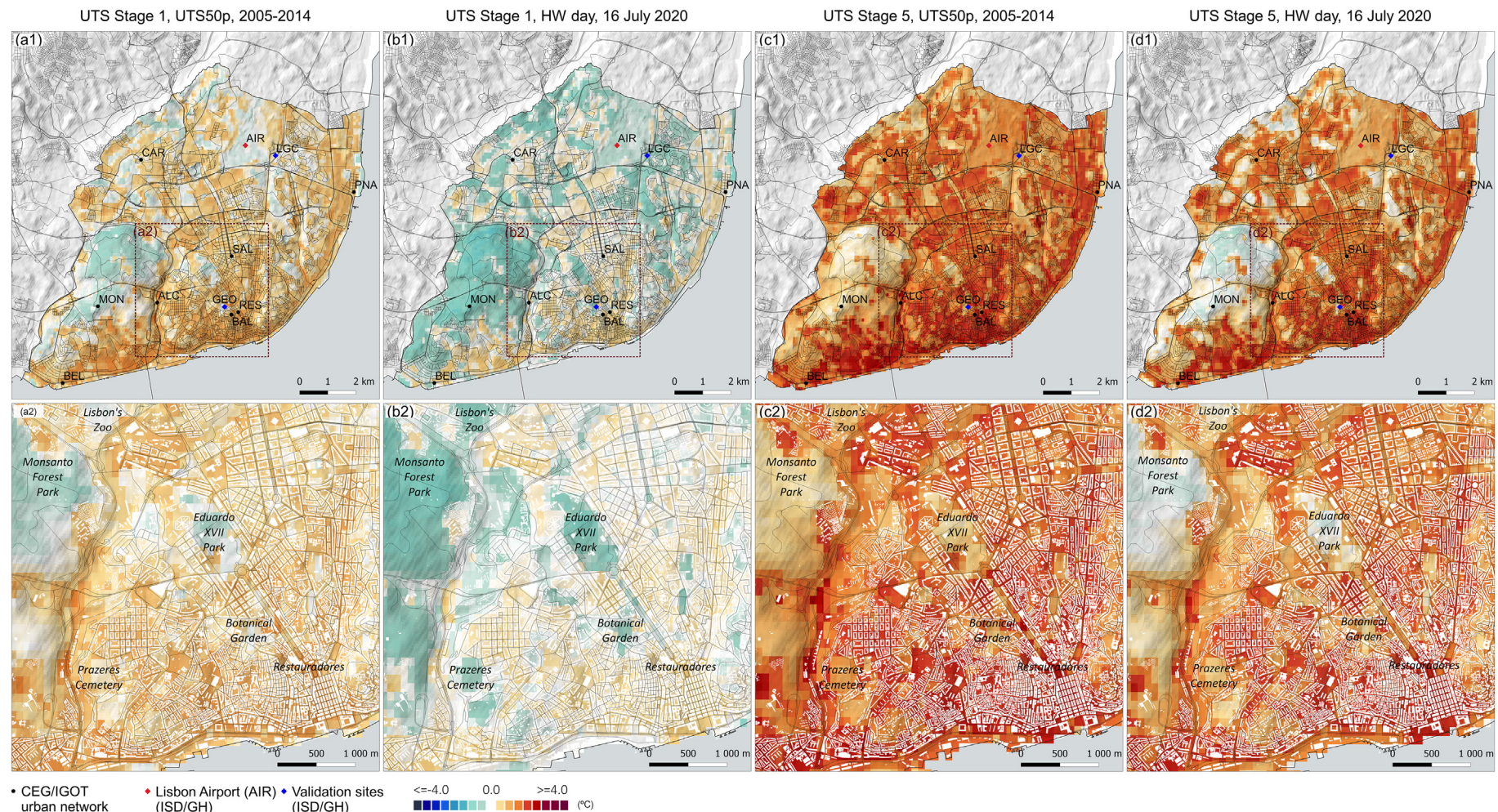


Fig. 2. Model predictions for the (a-b) nocturnal daily median UTS intensity (UTS Stage 1, from 11 p.m. to 6 a.m.), and (c-d) late afternoon daily maximum UTS intensity (UTS Stage 5, from 6 to 8 p.m.). In the upper row, city maps correspond to: (a1) and (c1) the pixel-wise 50th percentile (summer 2005–2014 time series); and (b1) and (c1) the warmest day of the 2020 heatwave (16th July). Below, corresponding zoom details are shown.

Table 3

Inputs to predict UTS intensity, based on scenarios.

| UTS Stage | Predictors | | | | | | | | | | | |
|----------------------|-------------------|----------------------|-----------------------------|----------------------------|----------------------|-----------------------|-------------------|----------------------|---------------------|---------------------------|--------------------------|--|
| | Tr (°C) | | | Tr_d2h (°C) | | | Ws (m/s) | | | LCZ _{BR} | | |
| 1 | 16 | 20 | 24 | 28 | 0.8 | 1.2 | 0.5 | 5.0 | 10.0 | No change | 3.5 | |
| 5 | 20 | 24 | 28 | 32 | 1.7 | 2.5 | 3.6 | 7.9 | 13.5 | No change | 3.5 | |
| Description | Cool ^a | Typical ^a | Present HW day ¹ | Future HW day ^b | Typical ^c | Elevated ^c | Weak ^a | Typical ^a | Strong ^a | Current City ^d | Denser City ^e | |
| Acronym ^f | A | B | C | D | 1 | 2 | a | b | c | - | f | |

^a Considering 1981–2010, 5th, 50th, and 95th percentiles of Tr and Ws, for the reference Lisbon Airport site time series (Lott, 2004).^b Considering 2081–2100, 95th percentile, with RCP8.5 scenario, as per (Parente et al., 2018), 6.9 °C above the 90th percentile of the Lisbon Airport site time series reference period 1981–2010 (Lott, 2004).^c Considering 1981–2010, 50th, and 90th percentiles of Tr_d2h, for the reference Lisbon Airport site time series (Lott, 2004).^d Present-day LCZ classes.^e Areas 'to-be-developed' turned into LCZ 2 (dense, midrise) class.^f Scenarios acronyms correspond to the concatenation of the UTS Stage predictors (e.g., a 'Future HW day', with 'Elevated' Tr_d2h, 'Typical' Ws and 'Current City' is named as 'UTS1_D2b'; the equivalent with 'Denser City' is 'UTS1_D2f').

alternative was calculated. All the inputs of these scenarios are shown in Table 3. The aim of these scenarios is to show the relative contributions of each predictor to the UTS intensity and how these affect the UTS spatial pattern.

Figs. 3 and 4, and corresponding online media files, represent the sequence of maps of these alternative weather-based scenarios (the 'Denser City' scenario is shown later), together with the UTS intensity predictions, in key locations. The complete list of scenarios, corresponding inputs is available in Tables S10 and S11, in Supplementary Materials Appendix A, and still frames of the resulting maps are available in Supplementary Materials, Appendix B.

Firstly, model results indicate that the overall air temperature level, as per the Tr input, affects the maximum UTS intensity inversely, as it decreases by approximately 0.4 °C, per each 10.0 °C of Tr increase. However, the combination of wind speed (Ws) and Tr_d2h have the greatest influence over the Lisbon's UTS spatial pattern. Accordingly, in the

absence of significative wind speeds (i.e., 'Weak' Ws scenarios), the 'Compact' areas become responsible for the positive UTS predictions, as multiplied by the Tr_d2h variable. As a result, the greater the 2-hour temperature change (Tr_d2h), the starker become the positive UTS intensities, in the most compact areas of the city. The topography contribution, under these 'Weak' Ws scenarios is only very slightly noticeable.

Contrariwise, as the regional wind speed augments, the UTS contrast between the leeward and windward locations accentuates – in the northernmost areas of the city, the UTS intensity is reduced due to the exposure to the regional northern winds; conversely, in the southernmost areas, the positive UTS becomes enhanced, resulting from the added contributions of both the topographic shelter and the urban compactness effects. Hence, during 'Strong' Ws conditions, northern neighbourhoods of the city tend to be cooler, compared to the city centre, and the positive UTS spatial pattern recedes to the southern/

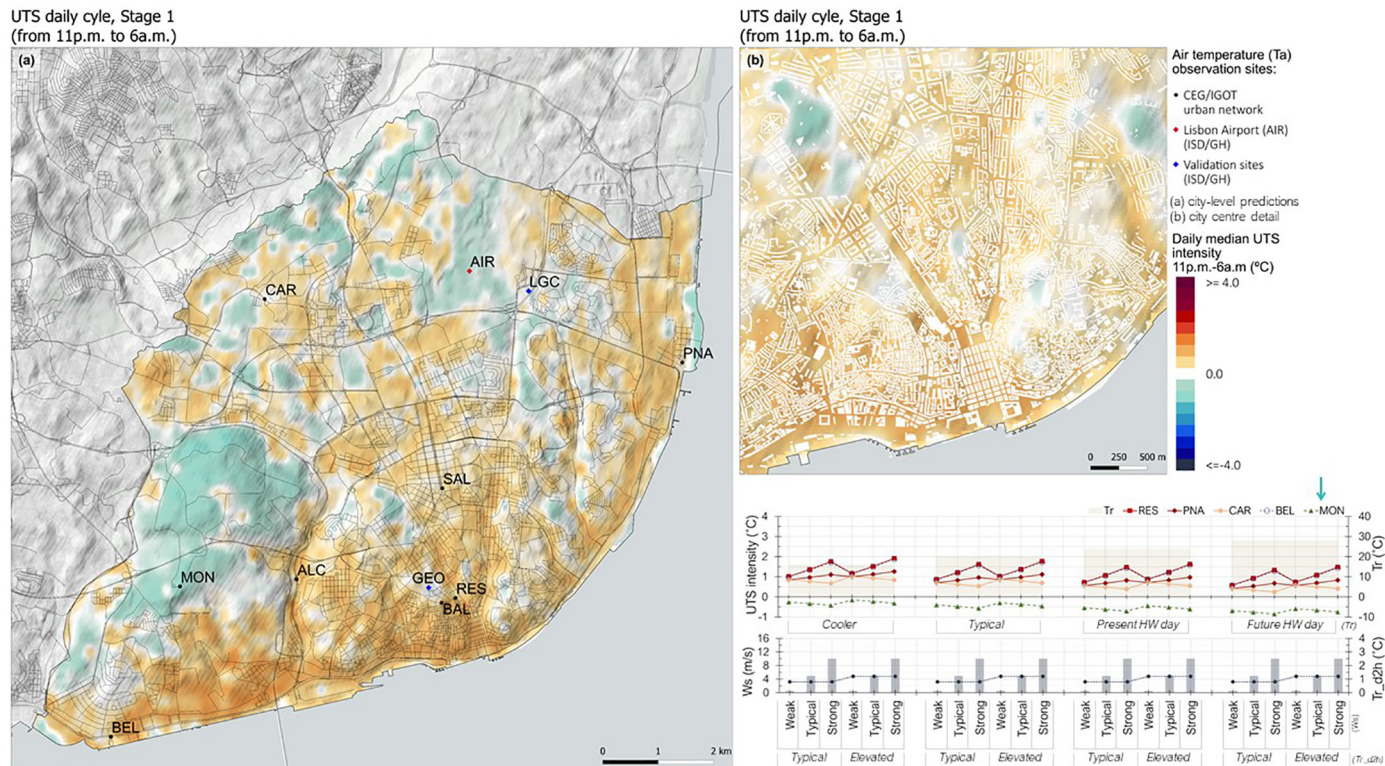


Fig. 3. Weather scenarios of current urban development status: model predictions of the nocturnal daily median UTS intensity (UTS Stage 1, from 11 p.m. to 6 a.m.) response to alternative combinations of input weather-related predictors. Still image shows the climate change scenario identified as UTS1_D2c (as per the concatenation of the Table 3 acronyms), considering a strong HW (percentile 95th), per RCP8.5 predictions in (Parente et al., 2018), as indicated on the top of the right hand-side plots. The media file of the full sequence is available online, through the still image link.

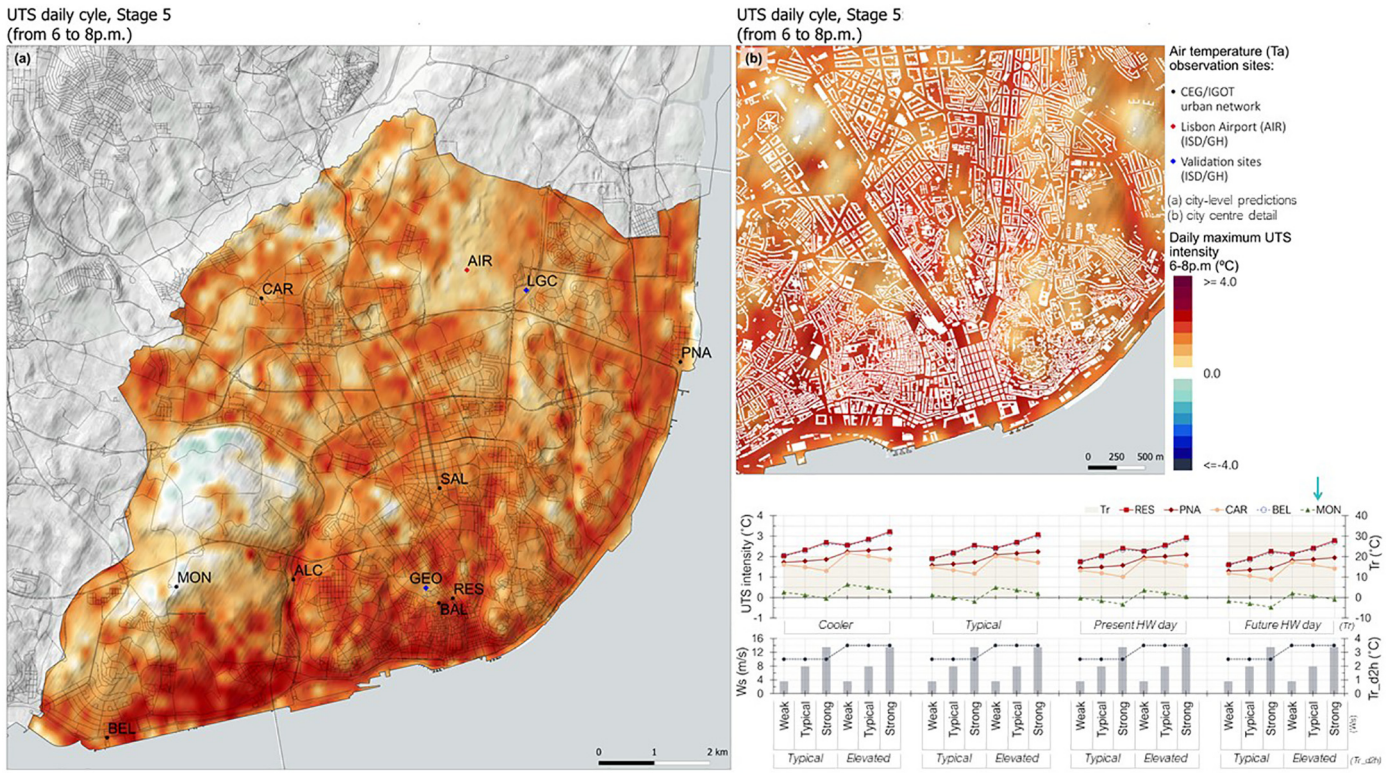


Fig. 4. Weather scenarios of current urban development status: model predictions of the daily late afternoon maximum UTS intensity (UTS Stage 5, from 6 p.m. to 8 p.m.) response to alternative combinations of input weather-related predictors. Still image shows the climate change scenario identified as UTSS_D2c (as per the concatenation of the Table 3 acronyms), considering a strong HW (percentile 95th), per RCP8.5 predictions in (Parente et al., 2018), as indicated on the top of the right hand-side plots. The media file of the full sequence is available online, through the still image link.

western riverside areas of the city. Maximum UTS values are predicted where: (i) topographic shelter is greater; and (ii) built-up compactness (LCZ_{BR}) is also greater. According to the model, under equal Tr and Tr_{d2h} scenarios, an increase of circa 4 m/s in the background/regional wind speed alone accounts for a 0.5 °C UTS intensity increase, at the city centre (Restauradores), during both UTS Stages.

Regarding the 'Present HW day' and 'Future HW day' scenarios, positive UTS intensities are predictor over fewer areas of the city, especially under calm conditions, when its intensity is lower than 1.7 °C, during the night (median), and lower than 3.0 °C, during the late afternoon (maximum), on every case. However, these are still significative anomalies given the background extreme temperatures during the night (median: 24 and 28 °C, respectively), and in the late afternoon peak (maximum: 28 and 32 °C, respectively).

Finally, the impacts of a 'Denser City', under a 'Future HW day' (climate change RCP8.5 scenario, 2081–2100 as per (Parente et al., 2018)) scenario are presented in Fig. 5. 'Elevated' Tr_{d2h} was used, as hourly temperature changes are usually greater under HW conditions (related with greater thermal amplitudes). The predicted UTS intensity was added to the background Tr of the corresponding UTS Stage, to obtain the absolute degrees of air temperature. While the maximum UTS value is not significantly different from the 'Present HW day' (in the Fig. 3 and Fig. 4 media files and Supplementary Materials, Appendix B), the 'Future HW day' with 'Denser City' scenario shows an expansion of the positive UTS intensities to the areas of the city in which future urban development is possible. The predictions indicate up to 1.0 °C of temperature increase, mostly in the northern, and eastern areas of the city. Furthermore, these areas are deemed the most critical in the city of Lisbon, not only because of the local UTS potential aggravation, but mostly because an upwind densification scenario is expected to further block the regional wind penetration in the city, enhancing the UTS at the city centre as well. Microscale modelling details of these areas can be found in (Lopes et al., 2020a). The cooling effect of

the 'to be consolidated' future green spaces is also detected, although they represent smaller areas.

4. Discussion

As described in (Oke et al., 2017), there are four main methods to obtain city-level air temperature data: (i) field observations; (ii) numerical models; (iii) physical models; and (iv) empirical models. While numerical and physical models have their main advantage in the fact that both allow quasi-controlled experiments and thorough description of outdoor thermal comfort levels (e.g. Geletič et al., 2018, 2021), they are harder to implement outside the academia, due to economic, logistic, expertise, or computational constraints (Oke et al., 2017). As such, these methods are usually not employed by the city-level public administration to compare the climate performance of future urban development prospective scenarios. On the other hand, field observations are easier to access and interpret, from readily available sources: they can be divided into in-situ and remote sensing measurements (Oke et al., 2017). The former, depicts air temperature observations as discrete values in space (i.e., data points), and the ability to produce rigorous high-resolution (sub-kilometric) urban air temperature maps (i.e., with enough spatial detail to ensure distinction between LCZ homogenous neighbourhoods) with this data depends on the density and reliability of the local weather stations network (Meier et al., 2015; Oke et al., 2017). While examples of high-density urban canopy layer weather networks exist (e.g. Milošević et al., 2021), they are not very common (Meier et al., 2015), many studies are using citizen acquired data to fill in this need, despite the data quality limitations, such as systematic positive bias in the results (Droste et al., 2020; Meier et al., 2015; Nopoly et al., 2018; Nipen et al., 2020). Still, air temperature observations can only be used for urban planning prospective studies if accompanied by measurable indicators of thermal performance.

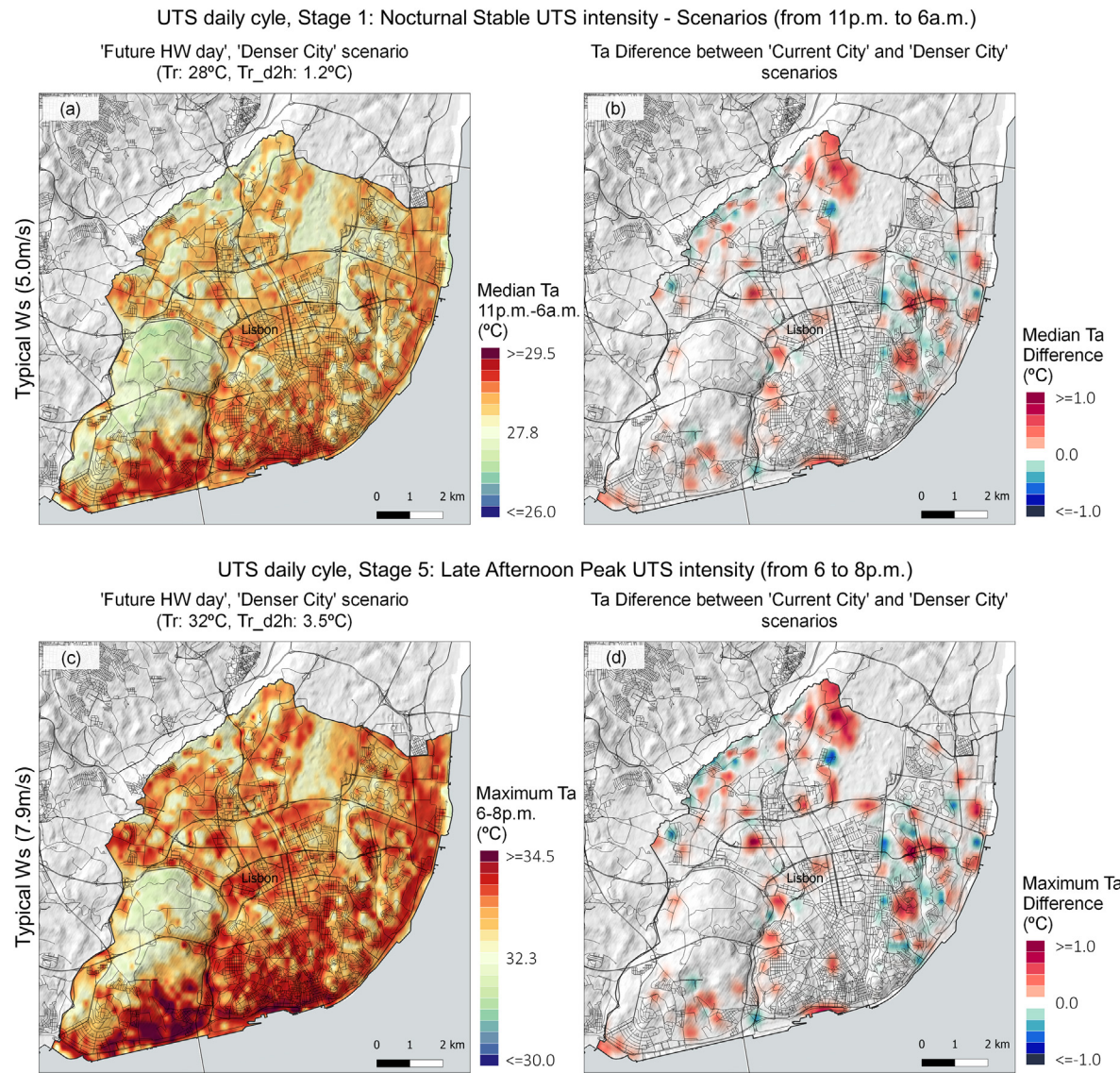


Fig. 5. Air temperature (Ta) model predictions for the 'Denser City' under a 'Future HW day' scenario, and Ta differences to an equivalent 'Current City' scenario: (a-b) nocturnal median (UTS Stage 1, from 11 p.m. to 6 a.m.); and (c-d) late afternoon maximum (UTS Stage 5, from 6 p.m. to 8 p.m.).

Empirical models, such as the one developed in this study, overcome some of this constraints, while considering the practical needs of local authorities in deploying a urban planning assessment model implementation (Oke et al., 2017). These depict the statistical relation between the variable of interest (here, the urban air temperature anomaly) and candidate predictor variables, and while they lack the decimal-level rigour of physics and numerical models, they provide a straightforward means for local authorities to simulate and decide upon results, without the need of an expert team or great computational capacity (Oke et al., 2017).

Still, one limitation of empirical models developed so far is the lack of integration of temporal variability, due to statistical methodology constraints (Gelman and Hill, 2006; Zuur et al., 2009a, 2009b). This statistical limitation is partially due to the absence of dense in-situ observation networks, as mentioned above – i.e., lack spatial sampling that leads to strong autocorrelation in the data (Gelman and Hill, 2006). More specifically, it is much more common to have UHI studies based on low density measurements, with long time series (e.g.), than the opposite, and this poses inter-class correlation issues that, in turn, make it difficult to overcome the violation of statistical modelling assumptions (independence, homogeneity). LM models are the most frequently used, both in UHI and surface UHI studies, and to overcome the

temporal-related constraints they usually focus on predicting the typical UHI magnitude, per time-fixed predictors such urban morphology, surface materials, geographic factors (Alcoforado and Andrade, 2006; Oke et al., 2017). While such results can be used by the local administration to establish the average effects of time-fixed predictors, they do not allow to disclose their interactions with the background weather.

Here, to fill in this gap, a LMM approach is implemented, using 10 years of data from a quality ensured mesoscale network (Alcoforado, 2013; Alcoforado et al., 2007; Lopes et al., 2013). Through this methodology, the site-specific variance is controlled by the introduction of the so-called "random effects", i.e., by partitioning the variance that is associated with each site's data, a technique very frequently used in other research domains, such as ecology and health (Gelman and Hill, 2006; Zuur et al., 2009a, 2009b), but not frequent in urban climate studies (Du et al., 2016). Hence, it allows to produce a time continuous model, that can be validated out of the temporal scope of the training dataset and implemented as a daily urban temperature monitoring tool (Gelman et al., 2010; Verbeke and Molenberghs, 2000; Zuur et al., 2009a, 2009b). A previous experience focusing on temporal-resolved urban air temperature models has been implemented by (Du et al., 2016). This study has successfully provided a local algorithm to predict surface temperature, based on satellite data and landscape composition

pixels. Even though the subject of this work is the land surface temperature (LST) (hence, the surface UHI), the authors describe how the LMM approach outperforms the LM equivalent model, both in terms of residuals and autocorrelation issues. In addition, a positive relation was established between the diurnal LST and the percentage of buildings, bare soil, and impervious surfaces (Du et al., 2016). A single example of LMM air temperature prediction model was found, in the urban climate literature, at the time of this study (as per the keywords and titles found in the google scholar and science direct databases): in (Parison et al., 2020), the authors have employed a LMM approach to model thermal comfort, as a function of watering strategies, indicating a reduction of up to 2.0 °C in the UTCL-equivalent temperature related to watered surface areas. However, this study only comprised two urban stations and focused in the microclimate impact.

Locally, it is possible compare results with previous empirical studies. In Lisbon, previous modelling attempts have been described in (Alcoforado and Andrade, 2006) indicating several wind-related patterns of the local so-called UHI, including a 'Wind-sheltered thermal pattern' related with 'N' wind days. Its results showed the broad spatial patterns of the Lisbon's nocturnal UHI intensity isotherms, depicting the riverside areas as where the thermal anomaly is greater, and Monsanto area as the coolest. The authors also suggested the impact of topography in sheltering the city from regional background winds, although the regression-wise model results indicated altitude has having the greatest contribution, regression-wise. More recently, the CEG/IGOT group collaborated with Lisbon's municipality in a local project called Lisbon's 2020 project "Cartography for Thermal Vulnerability – Mapping the effects of heatwaves in Lisbon" (translation from the Portuguese original "Cartografia de Vulnerabilidade Térmica - Mapeamento dos efeitos das ondas de calor em Lisboa, face às projeções climáticas") (Lopes et al., 2020b), where the 2005–2014 time series was used to test a bayesian regression kriging method (Krivoruchko, 2012), by the introduction of selected predictors, such as urban morphology indices (Correia, 2019) and Copernicus Land Monitoring Service layers (European Environment Agency (EEA), 2018c, 2018b). However, this work's usefulness was limited due to (i) the absence of coefficients/weights for each predictor (to evaluate the UTS sensitivity to changes in each indicator), and (ii) the inability to solve the UTS's temporal response to weather changes.

While the results from the current study agree with the above-mentioned findings (Alcoforado and Andrade, 2006; Lopes et al., 2020b), both in terms of the spatial pattern and the magnitude of the typical 'N' days nocturnal UTS intensity, new findings arise from the usage of weather predictors and estimating the relative weights that both geographical and urban density factors have, as they interact with background air temperature, wind speed or hourly air temperature changes. The urban development is found to be the strongest contributor to the Lisbon's UTS, proportionally to the 2-hours background air temperature change. Oke et al. (2017) has previously mentioned how the UHI effect is a result from the difference between the cooling rates at the rural and urban areas, which are greater in the former, and reduced in the latter (due to the thermal storage and thermal inertia of the urban materials), indicating a positive relation between daily thermal amplitude and the UHI intensity. While this effect is the result of the urban occupation, the authors have suggested that attention should be given to additional geographical/landscape control factors, such as local terrain or coastal proximity, as these may contribute to a so-called 'spurious' positive urban-rural difference, not attributable to the urban presence itself.

This study's model depicts an example of such complex interactions, in Lisbon, and allows to estimate corresponding urban and geographical, daily. Hence, all scenarios showed a positive UTS, at the city centre, during the summer 'N' days. While HW events seem to disaggregate the UTS, by 0.3 °C per each 1.0 °C background air temperature increase, there is, at least a circa 1.0 °C UTS intensity, during the night, under moderate wind speed and 2-hours air temperature change. However,

as the wind speed augments, the topographic exposure becomes increasingly important to the city's UTS spatial pattern, which recedes to the riverbank and valley areas, with peak intensities where the maximum topographic shelter and built-up compactness overlap. This wind speed-dependence is visible both in the present day and future climate change scenarios. Finally, while the UHI maps from previous studies were able to depict the overall urban pattern, the LMMf0 UTS maps provide an increased level of spatial detail, providing an urban thermal response assessment tool which is able to quantify the distinct contributions from either the LCZ classes, such as compact city-blocks or mid-sized urban parks, or the sheltering effect of local terrain to the prevailing northern winds.

Model results show that Lisbon's case study is an example of a city where the geographical effects have a strong contribution to the local urban thermal anomaly, quantified through the UTS approach. These forcing factors cannot be dissociated from urban geometry, while predicting the urban air temperature anomaly, a circumstance that has been discussed by (Oke et al., 2017).

Limitations from the current model are mostly related with available data constraints. Firstly, due to the scarcity of urban stations and their locations, no significant relation could be established with spatial coordinates, to include a proper spatial autocorrelation structure in the model. However, next steps of the research will include addressing this issue through the interpolation of model residuals. In addition, the sites are characterized by a strong agreement between the topography and built-up occupation - e.g. terrain elevation has a Pearson's correlation of 0.68 ($p\text{-value} < 0.01$), with an urban density index (Lopes et al., 2020b). Hence, it becomes problematic to introduce the wind speed interaction with both the urban compactness and topographic exposure predictors, simultaneously. In future works, the collinearity issue should also be addressed to account for the additional wind sheltering effect of the buildings. Two additional case-specific limitations are the absence of data on river and coastal breezes, as stated in a previous study (Oliveira et al., 2021), as well as the lack of high-resolution geospatial information readily available (e.g. building heights). Finally, while the assessment of future climate change scenarios might be helpful in guiding present-day urban planning adaptation measures, it should be noted that such future climate conditions might be outside of the scope of observations included in the training data. Accordingly, present-day relations might not hold true in the future. As such, current results should be viewed as scenarios for urban adaptation guidance, rather than forecasts.

Finally, it should be noted that empirical models should not be generalized to other locations, especially where circumstances are very different, as the estimations are case-specific. However, they provide a straightforward tool for the local regulators to contemplate potential urban development scenarios, and their impact on the Lisbon's urban climate. While the statistical assumptions that underline the most frequently used LM limit its usefulness, here, by combining both the time-fixed geographic/urban factors, and the time-varying weather predictors, it becomes possible to explore scenarios and estimate the corresponding sensitivity of the UTS intensity to their changes, and on a day-to-day basis.

Such strategies become most helpful while estimating the Lisbon's air temperature during the summer, especially under HW conditions, when a positive UTS is deemed more concerning. Hence, the Lisbon's summer and HW temporal-resolved empirical model provides a straightforward and helpful tool for local authorities to: (i) monitor daily changes in the city-level excess heat exposure; (ii) assess the corresponding human health vulnerability; and (iii) advise both short-term public health actions and long-term policy strategies. To the urban climate community at large, such results establish a precedent for (i) implementing similar LMM empirical model approaches; and (ii) integrating weather predictors and interaction terms whose influence over the time-fixed factors is expected to be statistically significant and meaningful. Future work will further re-assess the model, to validate its results out of the temporal scope of the input data as soon as

new (and denser) urban air temperature measurements become available, including the assessment of the spatial correlation in the residuals, and results comparison with kriging algorithms. In addition, it is the aim of the authors to further expand its usefulness, by establishing a framework to map and assess heat vulnerability, in Lisbon.

5. Conclusion

Air temperature is a key aspect of urban environmental health, especially in locations that are challenged by the prospects of enhanced HW, due to climate change. Lisbon is such a case, and while its local UHI effect has been studied for decades, previous spatial modelling attempts have been restricted to the typical seasonal conditions, as a response to urban geometry indicators, and geographic factors (river/coast distance and topography). This approach is also the most frequently used, in urban climate empirical studies. Hence, such models do not allow to infer day-to-day weather-related changes in the urban heat exposure. Here, to fill this gap, 10-year of air temperature data from Lisbon's mesoscale network (2005–2014), from June to September, are used to develop a LMM empirical approach to predict the local Urban Thermal Signal (UTS,), i.e., the sub-daily urban air temperature difference, compared to a non-urban reference site, according to the synchronous background/rural weather variables, as they interact with the local urban compactness and topography. Results show that the temporal-resolved LMM approach allows to accurately predict daily maps of the urban heat anomaly (late afternoon peak UTS, and nocturnal median UTS), at a 100×100 m spatial resolution. The UTS intensity is shown to have significant contributions from the interaction terms between the time-fixed factors and the time-varying weather predictors, ensuring mean absolute errors lower than 0.5–0.9 °C (nocturnal median and late afternoon daily maximum UTS, respectively), both in the testing and validation datasets.

The interaction between the background air temperature 2-hours changes (i.e., bi-hourly thermal amplitude) and the LCZ-based Bowen-ratio (BR) predictor (a proxy for urban compactness) is shown to have the strongest positive effect. Hence, on average, a positive UTS effect establishes whenever: (i) the background air temperature difference is greater than 1.0 °C, in 2-hours; and (ii) the urban fabric is of the type 'Compact' (i.e., LCZ 1–3, or BR ≥ 3). In leeward locations, this positive thermal anomaly is further enhanced by the interaction between the north-to-northwest (NNW) topographic exposure index (positive, if sheltered from NNW winds, negative, if otherwise) in proportion to the synchronous background wind speed. Thus, under calm conditions, the urban compactness contribution is strongly apparent in the Lisbon's nocturnal/late afternoon UTS pattern, and leeward and windward differences are small; inversely, as wind speed augments, Lisbon's NNW topographic shelter becomes increasingly noticed in the UTS pattern, and, in some instances, overcomes the urban fabric's contribution, by establishing a positive UTS, even in areas with lower built-up compactness. In addition, the LMM is also used to predict Lisbon's heat anomaly, under climate change 'worst-case-scenario' conditions (RCP8.5 and 95th percentile HW intensity, for the 2081–2100 period): maps of the future UTS are assessed, by comparing current urban development with an urban densification alternative. Results show the significant impact of the built-up compactness in future heat exposure, where UTS changes can reach up to 1.0 °C, compared to the present-day urban development situation. Conversely, urban areas converted into dense tree covered parks may become 1.0 °C cooler, indicating the important role of green areas to the city's future environmental health.

Locally, results from the current study allow, for the first time, to predict the urban heat exposure patterns in Lisbon, during typical summer days and HW events (NNW wind conditions), both present and future. The model provides local authorities with an efficient and straightforward solution to test the UTS impacts of alternative urban planning pathways. While empirical models are based on local conditions, their

conclusions should not be extrapolated to different geographic contexts, the method serves as an example of a temporal-resolved approach to produce a readily available tool for urban-related stakeholders. To the overall urban climate and urban public health community, the current study provides a precedent in developing and using a LMM approach, capable of predicting daily variations in the spatial pattern and intensity of the urban air temperature, most useful in the assessment of present-day and future heat vulnerability.

The following are the supplementary data related to this article.

Supplementary data to this article can be found online at <https://doi.org/10.1016/j.scitotenv.2021.147710>.

Funding

This work was supported by the "Fundação para a Ciência e Tecnologia (FCT) – Portugal", [Ph.D. grant number PD/BD/52304/2013].

CRediT authorship contribution statement

Ana Oliveira: Conceptualization, Methodology, Formal analysis, Software, Visualization, Investigation, Writing – original draft. **António Lopes:** Resources, Supervision, Writing – review & editing. **Ezequiel Correia:** Data curation, Writing – review & editing. **Samuel Niza:** Supervision, Writing – review & editing. **Amílcar Soares:** Supervision, Writing – review & editing.

Declaration of competing interest

The authors declare that they have no known competing financial interests or personal relationships that could have appeared to influence the work reported in this paper.

References

- Alcoforado, M.J., 1992. *O Clima da Região de Lisboa. Contrastes e Ritmos térmicos*, in: *Memórias Do Centro de Estudos Geográficos*.
- Alcoforado, M.J., 2013. Assessing and modeling the urban climate in Lisbon. *Geographical Information and Climatology* <https://doi.org/10.1002/9781118557600.ch5>.
- Alcoforado, M., Andrade, H., 2006. Nocturnal urban heat island in Lisbon (Portugal): main features and modelling attempts. *Theor. Appl. Climatol.* 84 (1–3), 151–159.
- Alcoforado, M.J., Andrade, H., Lopes, A., Oliveira, S., 2007. *A ilha de calor de Lisboa. Aquisição de dados e primeiros resultados estatísticos para aplicação ao ordenamento urbano*. *Geophilia - o Sentir e Os Sentidos Da Geografia*.
- Alcoforado, M.J., Andrade, H., Lopes, A., Vasconcelos, J., 2009. Application of climatic guidelines to urban planning. The Example of Lisbon (Portugal). *Landsc. Urban Plan* <https://doi.org/10.1016/j.landurbplan.2008.10.006>.
- Alcoforado, M.J., Lopes, A., Alves, E., Canário, P., 2014. *Lisbon Heat Island. Statistical Study (2004–2012)*. *Finisterra* 98. pp. 61–80.
- Alexander, L., Herold, N., 2016. *ClimPACT2 Indices and Software*.
- Bates, D., 2007. *Linear Mixed Model Implementation in lme4*. October.
- Bates, D., Sarkar, D., Bates, M.D., Matrix, L., 2007. *The lme4 Package*. October.
- Bates, D., Mächler, M., Bolker, B.M., Walker, S.C., 2015. Fitting linear mixed-effects models using lme4. *J. Stat. Softw.* <https://doi.org/10.18637/jss.v067.i01>.
- Beniston, M., Stephenson, D.B., Christensen, O.B., Ferro, C.A.T., Frei, C., Goyette, S., Halsnaes, K., Holt, T., Jylhä, K., Koffi, B., Palutikof, J., Schöll, R., Semmler, T., Woth, K., 2007. Future extreme events in European climate: an exploration of regional climate model projections. *Clim. Chang.* <https://doi.org/10.1007/s10584-006-9226-z>.
- Chapman, L., 2000. Assessing topographic exposure. *Meteorol. Appl.* <https://doi.org/10.1017/S1350482700001729>.
- Chrysoulakis, N., Grimmond, S., Feigenwinter, C., Lindberg, F., Gastellu-Etchegorry, J.P., Marconcini, M., Mitra, Z., Stagakis, S., Crawford, B., Olofson, F., Landier, L., Morrison, W., Parlow, E., 2018. Urban energy exchanges monitoring from space. *Sci. Rep.* <https://doi.org/10.1038/s41598-018-29873-x>.
- CML, 2012. *Plano Municipal de Lisboa*, Diário da República, 2a Série, no168 de 30 de agosto de 2012.
- Correia, E., 2019. *Mapas Climáticos Urbanos - Geometria e densidade urbana atual*.
- Droste, A.M., Heusinkveld, B.G., Fenner, D., Steeneveld, G.J., 2020. Assessing the potential and application of crowdsourced urban wind data. *Q. J. R. Meteorol. Soc.* <https://doi.org/10.1002/qj.3811>.
- Du, S., Xiong, Z., Wang, Y.C., Guo, L., 2016. Quantifying the multilevel effects of landscape composition and configuration on land surface temperature. *Remote Sens. Environ.* <https://doi.org/10.1016/j.rse.2016.02.063>.
- EEA, 2012. Climate Change, Impacts and Vulnerability in Europe 2012: An Indicator-based Report. European Environment Agency <https://doi.org/10.2800/66071>.

- Espírito Santo, F., De Lima, M.I.P., Ramos, A.M., Trigo, R.M., 2014. Trends in seasonal surface air temperature in mainland Portugal, since 1941. *Int. J. Climatol.* <https://doi.org/10.1002/joc.3803>.
- European Environment Agency (EEA), 2018a. Building Height 2012 [WWW Document]. URL <https://land.copernicus.eu/local/urban-atlas/building-height-2012>.
- European Environment Agency (EEA), 2018b. Tree Cover Density [WWW Document]. URL <https://land.copernicus.eu/pan-european/high-resolution-layers/forests/tree-cover-density>.
- European Environment Agency (EEA), 2018c. Imperviousness Density [WWW Document]. URL <https://land.copernicus.eu/pan-european/high-resolution-layers/impermeousness/status-maps/2015>.
- Feigenwinter, C., Vogt, R., Parlow, E., Lindberg, F., Marconcini, M., Frate, F. Del, Chrysoulakis, N., 2018. Spatial distribution of sensible and latent heat flux in the City of Basel (Switzerland). *IEEE J. Sel. Top. Appl. Earth Obs. Remote Sens.* <https://doi.org/10.1109/JSTARS.2018.2807815>.
- Founda, D., Santamouris, M., 2017. Synergies between urban heat island and heat waves in Athens (Greece), during an extremely hot summer (2012). *Sci. Rep.* <https://doi.org/10.1038/s41598-017-11407-6>.
- Geletič, J., Lehnert, M., Savić, S., Milošević, D., 2018. Modelled spatiotemporal variability of outdoor thermal comfort in local climate zones of the city of Brno, Czech Republic. *Sci. Total Environ.* <https://doi.org/10.1016/j.scitotenv.2017.12.076>.
- Geletič, J., Lehnert, M., Krč, P., Resler, J., Krayenhoff, E.S., 2021. High-resolution modelling of thermal exposure during a hot spell: a case study using PALM-4U in Prague, Czech Republic. *Atmosphere* <https://doi.org/10.3390/atmos12020175>.
- Gelman, A., Hill, J., 2006. Data Analysis Using Regression and Multilevel/hierarchical Models. *Data Analysis Using Regression and Multilevel/Hierarchical Models*. <https://doi.org/10.1017/cbo9780511790942.029>.
- Giorgi, F., 2005. Climate change prediction. *Clim. Chang.* <https://doi.org/10.1007/s10584-005-6857-4>.
- Heaviside, C., Vardoulakis, S., Cai, X.M., 2016. Attribution of mortality to the urban heat island during heatwaves in the West Midlands, UK. *Environ. Heal. A Glob. Access Sci. Source* <https://doi.org/10.1186/s12940-016-0100-9>.
- Ivajnščič, D., Kaligarič, M., Žiberna, I., 2014. Geographically weighted regression of the urban heat island of a small city. *Appl. Geogr.* <https://doi.org/10.1016/j.apgeog.2014.07.001>.
- Jiang, P., Liu, X., Zhu, H., Li, Y., 2019. Features of urban heat Island in mountainous Chongqing from a dense surface monitoring network. *Atmosphere* <https://doi.org/10.3390/atmos10020067>.
- Köppen, W., 1931. *Grundriss der Klimakunde*. Walter de Gruyter (doi:citeulike-article-id: 13966583).
- Krivoruchko, K., 2012. Empirical Bayesian Kriging Implemented in ArcGIS Geostatistical Analyst. *ArcUser*.
- L, A., N., H., 2015. ClimPACTv2: Indices and Software. Technical Report of the World Meteorological Organisation Commission for Climatology Expert Team on Sector-specific Climate Indices.
- Levermore, G.J., Parkinson, J.B., 2017. An empirical model for the urban heat island intensity for a site in Manchester. *Build. Serv. Eng. Res. Technol.* <https://doi.org/10.1177/0143624416659323>.
- Levermore, G., Parkinson, J., 2019. The urban heat island of London, an empirical model. *Build. Serv. Eng. Res. Technol.* <https://doi.org/10.1177/0143624418822878>.
- Levermore, G.J., Parkinson, J.B., Laycock, P.J., Lindley, S., 2015. The urban heat island in Manchester 1996–2011. *Build. Serv. Eng. Res. Technol.* <https://doi.org/10.1177/01436244141549388>.
- Leys, C., Klein, O., Dominicy, Y., Ley, C., 2018. Detecting multivariate outliers: use a robust variant of the Mahalanobis distance. *J. Exp. Soc. Psychol.* <https://doi.org/10.1016/j.jesp.2017.09.011>.
- Li, D., Bou-Zeid, E., 2013. Synergistic interactions between urban heat islands and heat waves: the impact in cities is larger than the sum of its parts. *J. Appl. Meteorol. Climatol.* <https://doi.org/10.1175/JAMC-D-13-021>.
- Lopes, A., 2003. Changes in Lisbon's urban climate as a consequence of urban growth. *Wind, Surface UHI and Energy Budget*.
- Lopes, A., Saraiva, J., Alcoforado, M.J., 2011. Urban boundary layer wind speed reduction in summer due to urban growth and environmental consequences in Lisbon. *Environ. Model. Softw.* <https://doi.org/10.1016/j.envsoft.2010.05.015>.
- Lopes, A., Alves, E., Alcoforado, M.J., Machete, R., 2013. Lisbon urban heat island updated: new highlights about the relationships between thermal patterns and wind regimes. *Adv. Meteorol.* <https://doi.org/10.1155/2013/487695>.
- Lopes, A., Fragoso, M., Correia, E., 2018. Contextualização climática (Cap. 3) e Cenarização bioclimática (Cap. 4), in: Plano Metropolitano de Adaptação Às Alterações Climáticas, Volume I – Definição Do Cenário Base de Adaptação Para a AML – Relatório Preliminar. AML, Lisbon, pp. 71–168.
- Lopes, A., Matias, M., Correia, E., Oliveira, A., Reis, C., 2020a. Identificação das Ilhas de Calor Urbano e simulação para as Áreas Críticas da Cidade de Lisboa, Fase 2 – Simulações microclimáticas de duas áreas críticas (Baixa e Alta de Lisboa): situação atual e projeções para o futuro com modificações no edificado. Lisboa.
- Lopes, A., Oliveira, A., Correia, E., Reis, C., 2020b. Identificação das Ilhas de Calor Urbano e simulação para as Áreas Críticas da Cidade de Lisboa, Fase 1 – Caracterização e cartografia das ilhas de calor atuais (+adenda). Lisboa.
- Lott, J.N., 2004. The Quality Control of the Integrated Surface Hourly Database. *Bulletin of the American Meteorological Society*.
- Lowry, W.P., 1977. Empirical estimation of urban effects on climate: a problem analysis. *J. Appl. Meteorol.* 16, 129–135.
- Meier, F., Fenner, D., Grassmann, T., Jänicke, B., Otto, M., Scherer, D., 2015. Challenges and benefits from crowdsourced atmospheric data for urban climate research using Berlin, Germany, as testbed. *ICUC9 - 9th Int. Conf. Urban Clim. jointly with 12th Symp. Urban Environ. Challenges*.
- Mihalakakou, G., Santamouris, M., Papanikolaou, N., Cartalis, C., Tsangrassoulis, A., 2004. Simulation of the urban heat island phenomenon in Mediterranean climates. *Pure Appl. Geophys.* <https://doi.org/10.1007/s00024-003-2447-4>.
- Milošević, D., Savić, S., Kresoja, M., Lužanin, Z., Šećerov, I., Arsenović, D., Dunjić, J., Matzarakis, A., 2021. Analysis of air temperature dynamics in the "local climate zones" of Novi Sad (Serbia) based on long-term database from an urban meteorological network. *Int. J. Biometeorol.* <https://doi.org/10.1007/s00484-020-02058-w>.
- Napoly, A., Grassmann, T., Meier, F., Fenner, D., 2018. Development and application of a statistically-based quality control for crowdsourced air temperature data. *Front. Earth Sci.* <https://doi.org/10.3389/feart.2018.00118>.
- Nipen, T.N., Seierstad, I.A., Lussana, C., Kristiansen, J., Hov, Ø., 2020. Adopting citizen observations in operational weather prediction. *Bull. Am. Meteorol. Soc.* <https://doi.org/10.1175/BAMS-D-18-0237.1>.
- Oke, T.R., 1987. Boundary Layer Climates. Second edition. Routledge <https://doi.org/10.1017/CBO9781107415324.004>.
- Oke, T.R., 1988. The urban energy balance. *Prog. Phys. Geogr.* <https://doi.org/10.1177/0391338801200401>.
- Oke, T.R., Mills, G., Christen, A., Voogt, J.A., 2017. *Urban climates*. Cambridge University Press.
- Oliveira, A., Lopes, A., Niza, S., 2020a. Local climate zones in five southern European cities: an improved GIS-based classification method based on Copernicus data. *Urban Clim.* 33. <https://doi.org/10.1016/j.uclim.2020.100631>.
- Oliveira, Ana, Lopes, A., Niza, S., 2020b. Local Climate Zones Datasets from Five Southern European Cities: Copernicus Based Classification Maps of Athens. vol. 31. Data Br, Barcelona, Lisbon, Marseille and Naples.
- Oliveira, A., Lopes, A., Correia, E., Niza, S., Soares, A., 2021. Heatwaves and summer urban heat islands: a daily cycle approach to unveil the urban thermal signal changes in Lisbon, Portugal. *Atmosphere* 12, 292. <https://doi.org/10.3390/atmos12030292>.
- Parente, J., Pereira, M.G., Amraoui, M., Fischer, E.M., 2018. Heat waves in Portugal: current regime, changes in future climate and impacts on extreme wildfires. *Sci. Total Environ.* <https://doi.org/10.1016/j.jscitotenv.2018.03.044>.
- Parison, S., Hendel, M., Royon, L., 2020. A statistical method for quantifying the field effects of urban heat island mitigation techniques. *Urban Clim.* <https://doi.org/10.1016/j.uclim.2020.100651>.
- Peel, M.C., Finlayson, B.L., McMahon, T.A., 2007. Updated world map of the Köppen-Geiger climate classification. *Hydrol. Earth Syst. Sci.* <https://doi.org/10.5194/hess-11-1633-2007>.
- R Development Core Team, R, 2011. R: A Language and Environment for Statistical Computing. R Foundation for Statistical Computing. <https://doi.org/10.1007/978-3-540-74686-7>.
- Ramamurthy, P., Li, D., Bou-Zeid, E., 2017. High-resolution simulation of heatwave events in New York City. *Theor. Appl. Climatol.* <https://doi.org/10.1007/s00704-015-1703-8>.
- Reis, C., Lopes, A., Correia, E., Fragoso, M., 2020. Local weather types by thermal periods: deepening the knowledge about Lisbon's urban climate. *Atmosphere* <https://doi.org/10.3390/ATMOS11080840>.
- Shi, Y., Katschner, L., Ng, E., 2018. Modelling the fine-scale spatiotemporal pattern of urban heat island effect using land use regression approach in a megacity. *Sci. Total Environ.* <https://doi.org/10.1016/j.jscitotenv.2017.08.252>.
- Stewart, I.D., Oke, T.R., 2012. Local climate zones for urban temperature studies. *Bull. Am. Meteorol. Soc.* <https://doi.org/10.1175/BAMS-D-11-00019.1>.
- Szymański, M., Kryza, M., 2012. Local regression models for spatial interpolation of urban heat island—an example from Wrocław, SW Poland. *Theor. Appl. Climatol.* <https://doi.org/10.1007/s00704-011-0517-6>.
- Tan, J., Zheng, Y., Tang, X., Guo, C., Li, L., Song, G., Zhen, X., Yuan, D., Kalkstein, A.J., Li, F., Chen, H., 2010. The urban heat island and its impact on heat waves and human health in Shanghai. *Int. J. Biometeorol.* <https://doi.org/10.1007/s00484-009-0256-x>.
- Team, A., 2009. ASTER Global DEM Validation. Ipdaac usgs gov4 accessed 28 July 2009. <https://doi.org/10.1002/ar.a.20400>.
- Tolika, K., 2019. Assessing heat waves over Greece using the Excess Heat Factor (EHF). *Climatic* <https://doi.org/10.3390/clt010009>.
- Verbeke, G., Molenberghs, G., 2000. *Linear Mixed Models for Longitudinal Data*. Springer Series in Statistics, Springer Series in Statistics. Springer, New York.
- Wang, Z.-H., Bou-Zeid, E., Smith, J.A., 2010. Application of a sensor network to study the energy budget in urban canopies. *Proceedings of 15th Symposium on Meteorological Observation and Instrumentation, Atlanta*.
- Wicki, A., Parlow, E., 2017. Multiple regression analysis for unmixing of surface temperature data in an urban environment. *Remote Sens.* <https://doi.org/10.3390/rs9070684>.
- Wicki, A., Parlow, E., Feigenwinter, C., 2018. Evaluation and modeling of urban heat island intensity in Basel, Switzerland. *Climate* <https://doi.org/10.3390/cli6030055>.
- Zhou, Y., Shepherd, J.M., 2010. Atlanta's urban heat island under extreme heat conditions and potential mitigation strategies. *Nat. Hazards* <https://doi.org/10.1007/s11069-009-9406-z>.
- Zuur, Alain F., Ieno, Elena N., Walker, Niel J., Saveiev, Anatoly A., Smith, Graham, M., 2009a. Limitations of linear regression. *Mixed Effects Models and Extensions in Ecology with R*.
- Zuur, A.F., Ieno, E.N., Walker, N.J., Saveliev, A. a, Smith, G.M., Ebooks Corporation, 2009b. *Mixed Effects Models and Extensions in Ecology with R - Mixed Effects Modelling for Nested Data*. Statistics for Biology and Health.